AN IMPROVED MULTIPYRANOMETER ARRAY FOR THE MEASUREMENT OF DIRECT AND DIFFUSE SOLAR RADIATION

Bruce K. Munger[1], Jeff S. Haberl[2], Ph. D., P.E.
Energy Systems Laboratory
Texas A & M University
College Station, Texas

ABSTRACT

This paper describes an improved multipyranometer array (MPA) for the continuous measurement of direct and diffuse solar radiation. The MPA described in this paper is an improvement over previously published MPA studies due several new features, including: the incorporation of an artificial horizon that prevents reflected ground radiation from striking the tilted sensors, and a routine that corrects the spectral response of photovoltaic-type sensors used in the MPA. An optimal procedure has also been developed that eliminates invalid data, which are inherent in the simultaneous solution of the solar equations from the four MPA sensors. In this paper a description of the NIST-traceable calibration facility is provided and results are presented that compare the improved MPA-predicted beam to side-by-side measurements from a precision Normal Incidence Pyrheliometer (NIP).

INTRODUCTION

In the later 1980s several large-scale energy conservation projects were initiated in the United States by utilities and government agencies that incorporated long-term, before-after hourly measurements of energy use, including the Texas LoanSTAR program (Claridge et al. 1991), the Energy Edge project (Diamond et al. 1992), and Pacific Gas and Electric's ACT[2] project (Koran et al. 1992). In these projects the methods used to calculate the measured energy conservation and retrofit savings varied from empirical regression models to calibrated simulation models. In the case where a calibrated simulation model is used to measure the energy retrofit savings it has been shown by Haberl et al. (1995) that the accuracy of a calibrated simulation model can improve substantially when the simulation is driven by a weather file containing locally measured weather data versus calibration efforts that are based on Typical Meteorological Year (TMY) weather data or other standard weather tapes. In buildings where solar effects are significant there is an additional improvement in simulation accuracy when locally measured beam and diffuse solar measurements are incorporated as well.

Until recently, the long-term recording of beam and diffuse solar measurements usually required either the use of very expensive microprocessor-based precision instruments that tracked the sun, or worse, precision instruments that needed constant manual adjustment to keep them continuously pointed at the sun. In most cases, it is rare to find accurately measured hourly beam and diffuse solar data that extends over several years and does not contain 10% or more missing data due to instrument mis-alignment.

---

[1] Graduate Research Assistant, Mechanical Engineering Department, Texas A & M University.

[2] Associate Professor, Department of Architecture, Texas A & M University.

Fortunately, several developments have lead to a relatively inexpensive, robust device that promises to be capable of providing long-term beam and diffuse solar measurements - the multipyranometer array (MPA). The earliest work on a MPA related device for measuring diffuse sky radiation was performed in Finland by M. Hämäläien et al. (1985). Further development on the MPA was performed in several countries including the United States where Perez (1986) presented a method for deriving beam radiation from a series of vertically mounted pyranometer, and in Israel where Faiman et al. (1988) refined the design of the MPA around four fixed pyranometers and defined a robust solution method that included an anisotropic diffuse sky model. Further advancements were made on the MPA in the United States by Curtiss (1990; 1992; 1993) who investigated different isotropic and anisotropic diffuse sky models, and devised several novel methods for solving the simultaneous MPA equations including an empirically-based statistical model, and artificial neural networks. Curtiss also made several recommendations for improving MPA measurements, including: (1) corrections for the spectral bias introduced by photovoltaic-based solar sensors, and (2), the use of an artificial horizon to eliminate the ground reflectance term which is unknown.

This paper reports on efforts to develop an improvement MPA including: (1) the addition of an artificial horizon, and (2) the development of a spectral correction for the photovoltaic-type solar sensor. Also, in the previous work by Curtiss (1990) and in the published MPA dataset that is contained in the ASHRAE Predictor Shootout (Kreider and Haberl, 1994a; 1994b) varying amounts of "invalid" data were reported that needed to be filtered-out of the MPA solution without recommendations regarding how to filter these data. This paper reports on the development of a procedure that automatically eliminates invalid data from the simultaneous solution of the solar equations from the four sensors. Results are presented from long-term side-by-side testing of the MPA-predicted data against measured 15-minute data provided by three precision instruments, including a thermopile-type Precision Spectral Pyranometer (PSP), a Shadow Band Pyranometer (SBP), and a Normal Incidence Pyrheliometer (NIP).

CURRENT WORK

The facility for testing the MPA is located at a university laboratory in central Texas. The test stand is situated on the south side of the laboratory building where the data from the sensors is collected by a data logger which is automatically polled weekly so data can be uploaded into a database.[3] Figure 1 is a photograph of the NIST-traceable test bench that shows the PSP (upper right), SBP, NIP, and MPA (lower left). Uniform black shields were used in back of each sensor to block the reflection from the wall directly to the north of the test stand. Figures 2a and 2b are photographs of the MPA including the proposed artificial horizon. The instrumentation used at the site is listed in Table 1.

The MPA consists of four photovoltaic-type solars sensors arranged so that each sensor sees a different portion of the sky that corresponds to the sun's path. The arrangement of the sensors in the current MPA is the same as the arrangement used by Curtiss (1990). The MPA that was

[3] This data collection effort is part of the LoanSTAR Monitoring program, an eight year $98 million revolving loan program. For additional information on the LoanSTAR program see Claridge et al. (1991). Recently, the solar test facility has been moved to the roof of the College of Architecture where additional testing and refinement can take place.

constructed uses four photovoltaic-type sensors, one sensor mounted horizontally, one 40 degree tilted sensor facing due south, one 40 degree tilted sensor facing 60 degrees east of south, and one 40 degree tilted sensor west of south as shown in Figure 2a and 2b. In Figure 2a the MPA is shown with the artificial horizon, in Figure 2b the MPA is shown without the artificial horizon. Both figures provide a view of the blackened shield that is used to uniformly block the reflected sunlight coming from the nearby white wall.

In order to test the device, the MPA-calculated beam and diffuse measurements were compared with measured data from NIST-traceable sensors capable of continuously measuring global horizontal radiation, diffuse solar radiation and direct-normal beam radiation. After the initial setup was calibrated and verified the data logger was set to 15-minute integration intervals for long-term measurements. Data quality was maintained through a combination of weekly polling and inspection plots, cross-checking of instrumentation using redundant measurements, and daily visual inspections of the instrumentation alignment (Munger and Haberl 1994).

RESULTS

The first correction that was developed for the MPA was to adjust for differences in the spectral response of the photovoltaic-type instrumentation used in the MPA and the more accurate NIST-traceable thermopile-type sensor. This difference in spectral response is produced by the different technologies that are used to measure solar radiation. In the precision sensor solar (i.e., the PSP) radiation is proportional to a millivolt output signal that is produced by a thermopile that is measuring the temperature difference between a blackened plate and a reference point within the shaded body of the instrument. A thermopile-type sensor produces a flat response to incident solar radiation. In the photovoltaic-type sensor solar radiation is proportional to the millivolt output produced by a calibrated photovoltaic sensor that is most sensitive to sunlight falling in the 0.5 and 1.0 um range as shown in Figure 3 (Duffie and Beckman 1991). Unfortunately, thermopile-type sensors are expensive, costing about five times as much as photovoltaic-type sensors, hence the motivation to use a corrected, photovoltaic-type sensor.

To correct for the spectral bias of photovoltaic-type sensors in the MPA a simple polynomial correction was developed as shown in Figure 4a, 4b, and 5. Previous efforts in this area by Michalsky et al. (1991) have also developed a more refined method. In general, the effect of the spectral response of the photovoltaic-type sensor is to over-predict solar radiation for insolation levels falling below 600 W/m^2, and under-predict solar radiation for levels above 600 W/m^2. This can be clearly seen in Figure 5 where the mid-day signal from the photovoltaic-type sensor can be seen dipping below the signal from the PSP. Correcting this with a sample polynomial expression improves the RMSE from 22.48 W/m^2 to 16.77 W/m^2 and improves the R^2 from 99.41% to 99.53% (Table 2). Figure 4b shows the corrected data from the photovoltaic-type sensor compared against the thermopile-type sensor. Figure 5 shows a daily profile of the data from the PSP along with the corrected and uncorrected data from the photovoltaic sensor.

The next step in the experimentation was to add an artificial horizon as shown in Figure 2a. In the previous work Curtiss (1993) recommended the use of an artificial horizon to eliminate the unknown reflected radiation from the ground. The addition of the artificial horizon reduced the unknown variables to two variables (i.e., beam radiation and the diffuse radiation) which creates a somewhat more stable solution as can be seen in Figure 6.

Unfortunately, there were still periods when the solution to the MPA equations produced unstable solutions. These periods are caused by cancellation errors in the geometric tilt factors of the beam and diffuse components. To improve this an additional filtering process was developed that automatically removed the invalid data from the MPA equations. Figure 7 shows the same data as Figure 6 after it has been passed through the MPA invalid data filtering routines. Additional information about the filtering routines can be found in Munger (1996).

Table 3 shows MPA-predicted beam radiation compared against beam radiation measured by the nearby NIP. In Table 3 results are shown for: a) MPA equations that utilized data directly from the photovoltaic-type sensors without spectral correction (Ib, T/C), b) MPA equations that utilized a spectral correction for the photovoltaic-type sensors (Spec Ib, T/C), c) MPA equations that utilized the invalid data filtering (Switch Ib, T/C), and d) MPA equations that used the spectral correction and invalid data filtering (Spec Switch, Ib, T/C). All MPA equations used the Temps-Coulson (1977) anisotropic diffuse sky model as recommended by Curtiss (1990).

In Table 3 it can be seen that the combination of a spectral correction and invalid data filtering improved the MPA beam predictions slightly from an RMSE of 113.5 W/m^2 (previously reported by Curtiss [1990]) to 104.5 W/m^2. Furthermore, what is most encouraging about the current results is that there is no longer any invalid data in the solution to the MPA equations. This feature is felt to be a significant enhancement to MPA development.

SUMMARY AND DISCUSSION

Side-by-side tests of MPA-predicted beam against NIP-measured beam solar radiation have been performed using long term 15-minute data in central Texas. Previously reported work with MPAs has been improved through the addition of a simple artificial horizon, spectral correction of the signal from the photovoltaic-type sensor, and development of an automated invalid data filtering procedure. These enhancements appear to have modestly improved the performance of the MPA over the previous results reported by Curtiss, and more significantly, appear to have resolved the issue of the automated removal of invalid data from the solution of the solar equations from the four solar sensors.

Additional testing of the MPA will continue at a new location located on the roof of the College of Architecture at Texas A&M that does not contain any nearby obstructions that plagued the previous location. Potential areas for refinement include optimizing the orientation of the MPA sensors, investigating the use of MPAs for solar beam and diffuse measurements in wildlife management, the use of MPAs for lighting measurements, and development of self-calibration checks for the MPA solar sensors.

ACKNOWLEDGMENTS

Support by the Texas State Energy Conservation Office through the LoanSTAR program is gratefully acknowledged. Special thanks for to the following people at the Energy Systems Lab for their assistance on this project: Dan Turner, Frank Scott, Curtis Boecker, Pat Tollefson, Kelly Miligan, Robert Sparks, and Ron Chambers. Thanks also to Peter Klima and Victor Kootin-Sanwu for assistance with the test bench.

REFERENCES

Claridge, D., Haberl, J., O'Neal, D., Heffington, W., Turner, D., Tombari, C., Roberts, M., Jaeger, S., 1991. "Improving Energy Conservation Retrofits with Measured Results". ASHRAE Journal, Vol. 33, No. 10, pp. 14-22, (October).

Curtiss, P. 1990. "An Analysis of Methods for Deriving the Constituent Insolation Components from Multipyranometer Array Measurements", Masters Thesis, Joint Center for Energy Management (February).

Curtiss, P. 1992. "An Analysis of Methods for Deriving the Constituent Insolation Components from Multipyranometer Array Measurements", Proceedings of the 1992 ASES/JSEE/KSES Solar Energy Engineering Conference, Maui, Hawaii, pp. 109-117.

Curtiss, P. 1993, "An Analysis of Methods for Deriving the Constituent Insolation Components from Multipyranometer Array Measurements", Journal of Solar Energy Engineering, Vol. 115, pp. 11-21.

Duffie, J.A. and Beckman, W.A. 1991. Solar Engineering of Thermal Processes, Wiley-Interscience, Madison, Wisconsin.

Diamond, R., Piette, M. Nordman, O., and Harris, J. 1992. "The Performance of the Energy Edge Buildings: Energy Use and Savings", Proceedings of the 1992 ACEEE Summer Study on Energy Efficient Buildings.

Eppley Laboratory, Inc., (1996) 12 Sheffield Ave., P.O. Box 419, Newport, R.I., 02840.

Faiman, D., Zemel, A. and Zangvil, A. 1988. "A method for monitoring Insolation in Remote Regions", Solar Energy, Vol. 39, pp. 327-333.

Haberl, J., Bronson, D., O'Neal, D. 1995. "An Evaluation of the Impact of Using Measured Weather Data Versus TMY Weather Data in a DOE-2 Simulation of an Existing Building in Central Texas." ASHRAE Transactions Technical Paper no. 3921, Vol. 101, Pt. 2 (June).

Hämäläien, M., Nurkkanen, P., and Salen, T., 1985. "A Multisensor Pyranometer for determination of the Direct Component and Angular Distribution of Solar Radiation", Solar Energy, Vol. 35, pp. 511-525.

Koran, W., Kaplan, M. and Steele, T. 1992. "DOE-2.1C Model Calibration With Short-Term Tests versus Calibration With Long-Term Monitored Data", Proceedings of the 1992 ACEEE Summer Study on Energy Efficient Buildings.

Kreider, J. and Haberl, J. 1994a. "Predicting Hourly Building Energy Usage: The Great Energy Predictor Shootout: Overview and Discussion of Results", ASHRAE Transactions Predicting Hourly Building Energy Usage: Technical Paper, Vol. 100, Pt. 2, (June).

Kreider, J. and Haberl, J. 1994b. "Predicting Hourly Building Energy Usage: The Results of the 1993 Great Energy Predictor Shootout Identify the Most Accurate Method for Making Hourly Energy Use Predictions", ASHRAE Journal, pp. 72-81 (March).

LI-COR Inc. (1996), 4421 Superior St., P.O. Box 4425, Lincoln, NE, 68504.

Michalsky, J., Perez, R., Harrison, L. and LeBaron, B. 1991. "Spectral and Temperature Corrections of Silicon Photovoltaic Radiation Detectors", Solar Energy, Vol. 47, No. 4, pp. 299-305. 5.

Munger, B., Harberl, J. 1994. "An Improved Multipyranometer Array for the Measurement of Direct and Diffuse Solar Radiation", Proceedings of the Ninth Symposium on Improving Building Systems in Hot and Humid Climates, Dallas, TX, pp. 125-131 (May).

Munger, B. 1996. "An Improved Multipyranometer Array for the Measurement of Direct and Diffuse Solar Radiation", Master's Thesis, Department of Mechanical Engineering, Texas A&M University, in preparation.

Perez, R., Seals, R. and Stewart, R. 1986. "On Estimating Beam Irridiance from Vertically Mounted Sensors", Proceedings of the 1986 Annual ASES Meeting, Boulder, Co, pp. 180-183.

Temps, R. and Coulson, J. 1977. "Solar Radiation Incident Upon Slopes of Different Orientations," Solar Energy, Vol. 19, pp. 179-184.

Table 1: Instrumentation used at the solar test bench.

Mfg.	Instrument	Mfg. Stated Accuracy
Eppley Labs	Precision Spectral Pyranometer (PSP)	± 0.5% from 0-2800 W/m^2
Eppley Labs	Normal Incidence Pyrheliometer (NIP)	± 0.5% from 0-2800 W/m^2
Eppley Labs	Shadow Band with Black & White Pyranometer (SBP)	± 1.0% from 0-1400 W/m^2
LI-COR	LI-200SA Pyranometer Sensor	± 3.0% from 0-3000 W/m^2

NOTE: The NIP, PSP, SBP, and Licors were all calibrated at the respective manufacturer's facilities (Eppley 1996, LI-COR 1996). The NIP on 2/10/93, the PSP on 10/16/92, the SBP on 2/23/93, and the Licors on 9/15/92.

Table 2: Comparison of PSP to Photovoltaic-type Sensor Measurements.

	Without spectral correction	**With spectral correction**
RMSE	22.48 W/m^2	16.77 W/m^2
$\mathbf{R^2}$	99.41%	99.53%

NOTE: Data shown are for 4,000 randomly selected data points from 15-minute data taken over a one year period in 1994.

Table 3: Comparison of MPA-predicted Beam Radiation Against NIP Measurements.

	Ib, T/C	**Spec Ib, T/C**	**Switch Ib, T/C**	**Spec. Switch Ib, T/C**
Spring				
RMSE (W/m^2)	272.2	290.6	109.9	111.1
R^2 (%)	70.5	64.2	93.5	93.5
% Invalid (%)	54.0	54.0	0.	0
Summer				
RMSE (W/m^2)	187.5	178.0	118.5	109.7
R^2 (%)	86.9	93.1	85.5	92.5
% Invalid (%)	16.6	16.6	0	0
Fall				
RMSE (W/m^2)	204.4	181.4	100.5	99.2
R^2 (%)	86.9	85.5	93.1	93.2
% Invalid (%)	45.8	45.8	0	0
Winter				
RMSE (W/m^2)	938.8	741.4	191.4	97.9
R^2 (%)	70.4	64.1	93.5	95.3
% Invalid (%)	46.2	46.2	0	0
Average				
RMSE (W/m^2)	400.7	347.9	130.1	104.5
R^2 (%)	78.7	76.7	91.4	93.6
% Invalid (%)	40.7	40.7	0	0

Table 4: MPA-predicted Beam from by Curtiss (1990)

Fixed albedo	% invalid (%)	RMSE (W/m^2)	R^2(%)
0.25	54.0	113.6	93.2
0.5	48.0	111.5	92.9
0.75	48.0	109.5	92.6

NOTE: Information presented utilized Temps Coulson and uniform ground reflectance.

Figure 1: Solar Test Bench at the Energy Systems Lab

Figure 2a: MPA with Artificial Horizon and Wall Shield

Figure 2b: MPA without Artificial Horizon

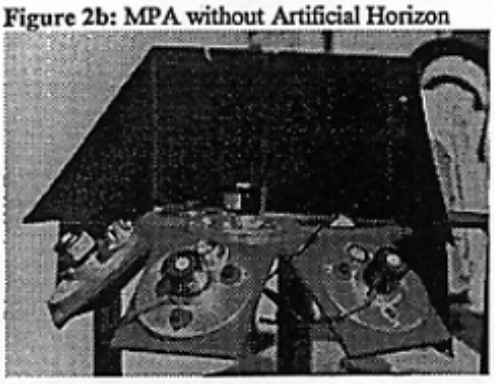

Figure 1: Solar Test Bench at the Energy Systems Lab
Figure 2: MPA with Artificial Horizon and Wall Shield
Figure 2b: MPA without Artificial Horizon

Figure 3: Relative Spectral Response of Thermopile Sensor, and Photovoltaic-type Sensor vs. the Solar Spectrum. (Source: Manufacturer's Manuals).

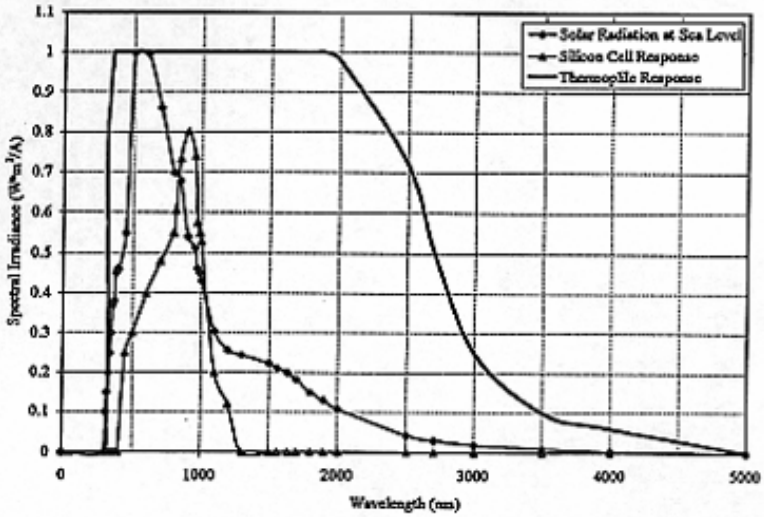

Figure 4a: PSP vs Photovoltaic-type Sensor Without Spectral Correction.

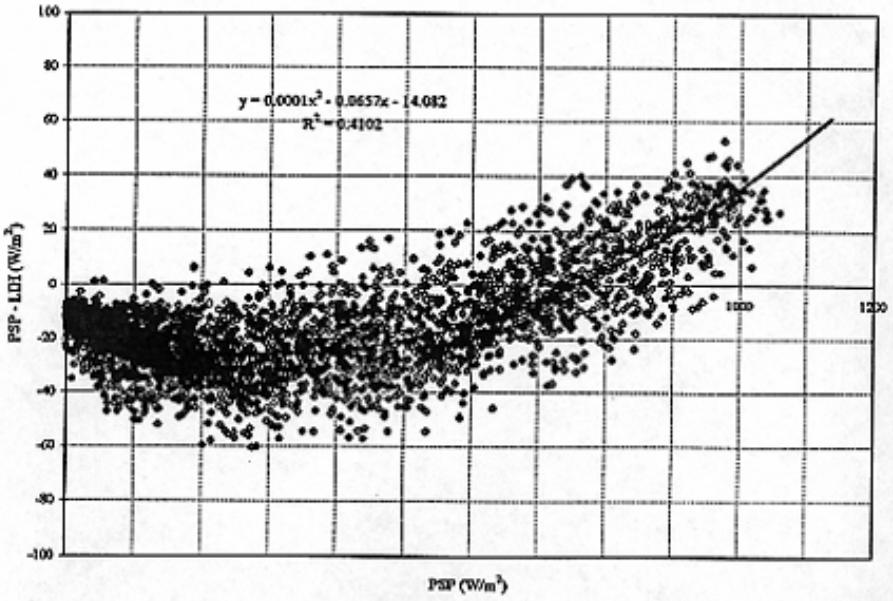

Figure 3: Relative Spectral Response of Thermopile Sensor, and Photovoltaic-type Sensor vs.

the Solar Spectrum. (Source: Manufacturer's Manuals).
Figure 4a: PSP vs. Photovoltaic-type Sensor Without Spectral Correction.

Figure 4b: PSP vs Photovoltaic-type Sensor With Spectral Correction.

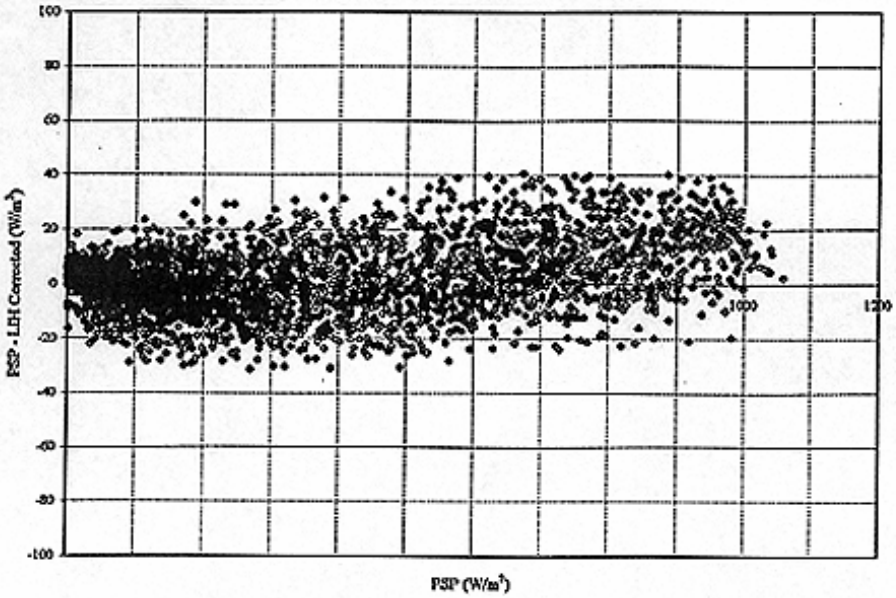

Figure 5: Global Horizontal Radiation from PSP & Photovoltaic-type Sensor With and Without Spectral Correction.

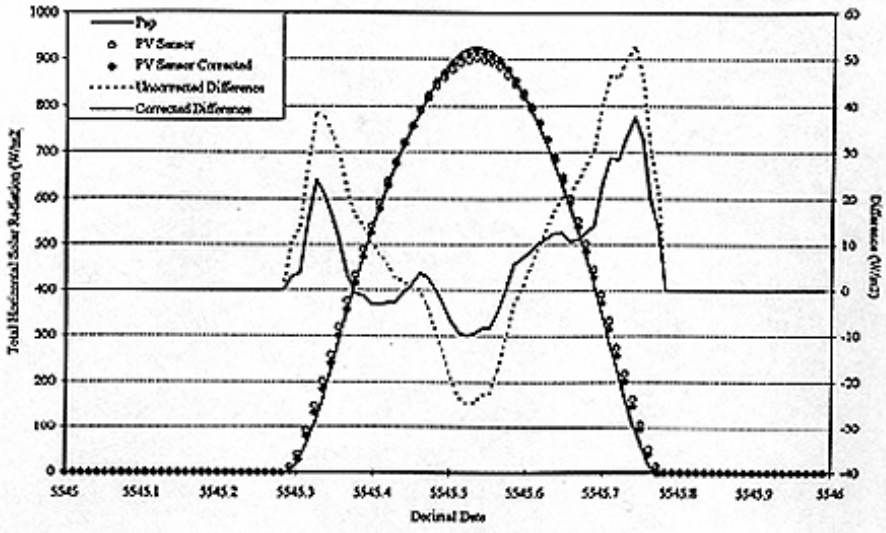

Figure 4b: PSP vs. Photovoltaic-type Sensor With Spectral Correction.
Figure 5: Global Horizontal Radiation from PSP & Photovoltaic-type Sensor With and

Without Spectral Correction.

Figure 6: Normal beam radiation predicted by the MPA (before filtering for invalid data).

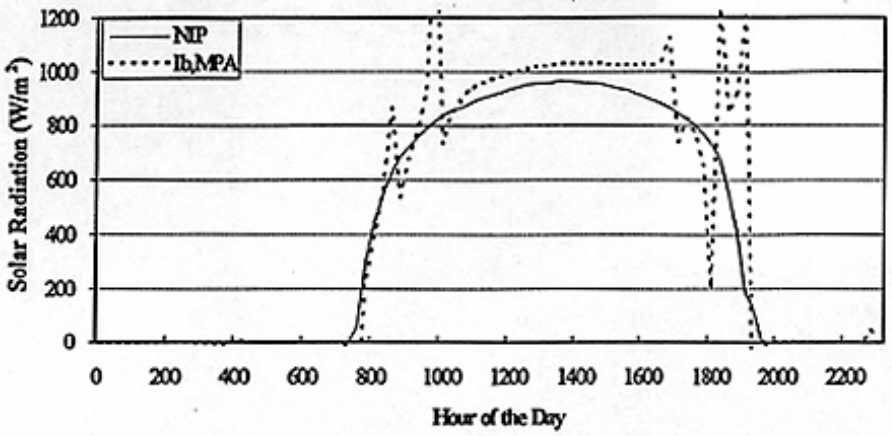

Figure 7: Normal beam radiation predicted by the MPA (after filtering for invalid data).

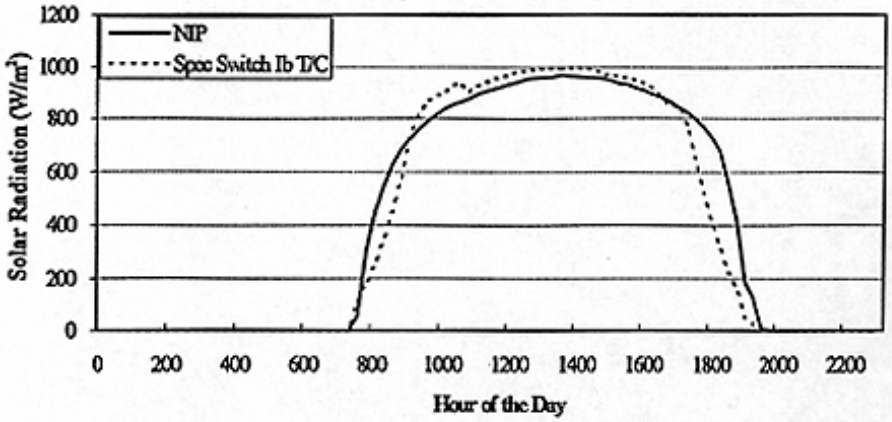

Figure 6: Normal beam radiation predicted by the MPA (before filtering for invalid data).
Figure 7: Normal beam radiation predicted by the MPA (after filtering for invalid data).

MPA EQUATIONS

Nomenclature

$I_{T,h}$ = Total radiation measured on the horizontal (W/m^2)
$I_{T,se}$ = Total radiation measured on the east of south facing tilted surface (W/m^2)
I_{Ts} = Total radiation measured on the south facing tilted surface (W/m^2)
$I_{T,sw}$ = Total radiation measured on the west of south facing tilted surface (W/m^2)
$I_{b,n}$ = Normal beam radiation (W/m^2)
$I_{d,h}$ = Diffuse radiation measured on the horizontal (W/m^2)
$R_{b,h}$ = Beam coefficient for horizontal
$R_{b,se}$ = Beam coefficient for east of south
$R_{b,s}$ = Beam coefficient for south
$R_{b,sw}$ = Beam coefficient for west of south
$R_{d,sc}$ = Diffuse coefficient for east of south
$R_{d,s}$ = Diffuse coefficient for south
$R_{d,sw}$ = Diffuse coefficient for west of south
$R_{r,se}$ = Reflection coefficient for east of south
$R_{r,s}$ = Reflection coefficient for south
$R_{r,sw}$ = Reflection coefficient for west of south
θ_1 = Incidence angle of beam radiation
β = collector tilt angle
γ = off-south azimuth angle
dec = decimal date
n = day of year
ϕ = latitude
ρ = foreground reflectance

$$\delta = \text{declination} = 23.45\, x \sin\left(360 \bullet \frac{284 + n}{365}\right)$$

Hour angle (ω) calculation:
at = 0.001868 · cos(β · π/180)
bt = 0.032077 · sin(β · π/180)
ct = 0.014615 · cos(2 · β · π/180)
dt = 0.04089 · sin(2 · β · π/180)
E = (229.2 · (0.000075+at-bt-ct-dt))
lcorr = ((90-96.55) ·4)
timefix = (lcorr+E)
soldec = dec+(timefix/(24·60))
ω = hour angle = (soldec - (int(soldec) + 0.5)) ·24·15

The equation for the total solar radiation incident upon the horizontal MPA sensor is:

$$I_{T,h} = I_{b,n} \cdot R_{b,h} + I_{d,h} \qquad (1)$$

The equation for the total solar radiation incident upon the east of south facing tilted MPA sensor is:

$$I_{T,se} = I_{b,n} \cdot R_{b,se} + R_{d,se} + I_{T,h} \cdot \rho \cdot R_{r,se} \quad (2)$$

The equation for the total solar radiation incident upon the south facing tilted MPA sensor is:

$$I_{T,s} = I_{b,n} \cdot R_{b,s} + R_{d,s} + I_{T,h} \cdot \rho \cdot R_{r,s} \quad (3)$$

The equation for the total solar radiation incident upon the west of south facing tilted MPA sensor is:

$$I_{T,sw} = I_{b,n} \cdot R_{b,sw} + R_{d,sw} + I_{T,h} \cdot \rho \cdot R_{r,sw} \quad (4)$$

The beam coefficients (R_b's) are calculated from:

$$R_{b,h} = \cos(\theta_z) = \cos(\theta_{i,h}) \quad (5)$$

$$R_{b,se} = \cos(\theta_{i,se}) \quad (6)$$

$$R_{b;s} = \cos(\theta_{i,s}) \quad (7)$$

$$R_{b,sw} = \cos(\theta_{i,sw}) \quad (8)$$

The diffuse coefficients (R_d's) are calculated from the Temps/Coulson (1977) model and are:

$$R_{d,se} = \frac{1+\cos(\beta_{se})}{2} \bullet \left[1+\sin^3\left(\frac{\beta_{se}}{2}\right)\right] \bullet \left[1+\cos^2(\theta_{i,se} \bullet \sin^3(\theta_z))\right] \quad (9)$$

$$R_{d,s} = \frac{1+\cos(\beta_{s})}{2} \bullet \left[1+\sin^3\left(\frac{\beta_{s}}{2}\right)\right] \bullet \left[1+\cos^2(\theta_{i,s} \bullet \sin^3(\theta_z))\right] \quad (10)$$

$$R_{d,w} = \frac{1+\cos(\beta_{sw})}{2} \bullet \left[1+\sin^3\left(\frac{\beta_{sw}}{2}\right)\right] \bullet \left[1+\cos^2(\theta_{i,sw} \bullet \sin^3(\theta_z))\right] \quad (11)$$

The incidence angles (θ_i's) in the previous equations are determined from the following:

$$\cos(\theta_z) = \cos(\theta_{i,h}) = \cos(\phi)\cos(\omega) + \sin(\phi)\sin(\delta) \quad (12)$$

$$\cos(\theta_{i,se}) = \sin(\delta)\sin(\phi)\cos(\beta_{se}) - \sin(\delta)\cos(\phi)\sin(\beta_{se})\cos(\gamma_{se}) + \cos(\delta)\cos(\phi)\cos(\beta_{se})\cos(\omega) + \cos(\delta)\sin(\phi)\sin(\beta_{se})\cos(\gamma_{se})\cos(\omega) + \cos(\delta)\sin(\beta_{se})\sin(\gamma_{se})\sin(\omega) \quad (13)$$

$$\cos(\theta_{i,s}) = \sin(\delta)\sin(\phi)\cos(\beta_{s}) - \sin(\delta)\cos(\phi)\sin(\beta_{s})\cos(\gamma_{s}) + \cos(\delta)\cos(\phi)\cos(\beta_{s})\cos(\omega) + \cos(\delta)\sin(\phi)\sin(\beta_{se})\cos(\gamma_{s})\cos(\omega) + \cos(\delta)\sin(\beta_{s})\sin(\gamma_{s})\sin(\omega) \quad (14)$$

$$\cos(\theta_{i,sw}) = \sin(\delta)\sin(\phi)\cos(\beta_{sw}) - \sin(\delta)\cos(\phi)\sin(\beta_{sw})\cos(\gamma_{sw}) + \cos(\delta)\cos(\phi)\cos(\beta_{sw})\cos(\omega) + \cos(\delta)\sin(\phi)\sin(\beta_{sw})\cos(\gamma_{sw})\cos(\omega) + \cos(\delta)\sin(\beta_{sw})\sin(\gamma_{sw})\sin(\omega) \quad (15)$$

Due to the use of the artificial horizon, the $I_{T,h}$ ρR terms in the equations for the tilted sensors is zero. Therefore, these four equations can be solved for the two unknowns, $I_{d,h}$ and $I_{b,n}$. Perez (1986) showed the beam radiation incident upon a surface can be determined using only two sensors. A procedure for solving this system of four equations with only two unknowns (i.e., overdetermined) has been developed by Munger (1996).